indirect study, coal was oxidatively degraded with sodium dichromate and the esterified products were identified as benzo- and dibenzothiophene derivatives by mass spectral analysis. The investigators concluded (*17*, p. 380) that "thiophene derivatives must be indigenous to coal." The direct XANES results reported here support these conclusions.

Simulations carried out with other model compounds yielded spectra that bore little resemblance to the coal spectrum. For example, simulations that used sulfate as the inorganic component yielded incorrect relative intensities for the absorptions at 3.0 and 11.8 eV, together with peaks at 15.0, 17.4, and 27.1 eV that are not present in the coal spectrum (*18*). Simulations with other organic models shown in Fig. 1 and in other ratios yielded peak positions or intensities, or both, that did not correspond to those observed in the coal spectrum. We therefore conclude that the thiophene unit is the most likely candidate as the main organic sulfur functional group in this particular coal.

The results described above illustrate the applicability and usefulness of high-resolution x-ray absorption spectroscopy, based on the use of intense synchrotron radiation for direct, nondestructive determination of the nature of organic sulfur in coal. It remains to be determined how sulfur in coal transforms through natural and various thermochemical processes during coal conversion and combustion. We expect that, by signal-averaging multiply scanned spectra, it will be possible to improve the signal-to-noise ratio shown in Fig. 3a so that quality spectra in the EXAFS region at high energy may be obtained and analyzed to complement the near-edge data.

C. L. SPIRO
J. WONG
Corporate Research and Development, General Electric Company, Post Office Box 8, Schenectady, New York 12301
F. W. LYTLE
R. B. GREEGOR
Boeing Company, Post Office Box 3999, Seattle, Washington 98124
D. H. MAYLOTTE
S. H. LAMSON
Corporate Research and Development, General Electric Company

References and Notes

1. J. N. Chakrabarti, in *Analytical Methods for Coal and Coal Products*, C. Karr, Ed. (Academic Press, New York, 1978), vol. 1, pp. 280–321; A. Attar, *ibid.*, vol. 3, pp. 585–622.
2. A. Attar and F. Dupuis, *Prepr. Am. Chem. Soc. Fuel Div.* **23** (No. 1), 214 (1978).
3. L. A. Harris and C. S. Yust, *Adv. Chem. Ser.* **192**, 321 (1981); V. Valkovic, *Trace Elements in Coal* (CRC Press, Cleveland, 1983), vol. 1, pp. 107–113, and references therein.
4. L. R. Ember, *Chem. Eng. News* **59** (No. 37), 20 (1983).
5. R. W. Bryers, Ed., *Ash Deposits and Corrosion Due to Impurities in Combustion Gases, Proceedings of International Conference* (Hemisphere, Washington, D.C., 1978).
6. C. W. Gehrs, D. S. Shriner, S. E. Herbes, E. J. Salmon, H. Perry, *Chemistry of Coal Utilization, 2nd Supplementary Volume*, M. A. Elliot, Ed. (Wiley, New York, 1981), chapter 31, p. 2159.
7. R. A. Dalla Batta, A. G. Piken, M. Shelef, *J. Catal.* **40**, 173 (1975).
8. T. L. Thompson and F. B. Raymer, in *Chemistry of Coal Utilization, 2nd Supplementary Volume*, M. A. Elliot, Ed. (Wiley, New York, 1981), chapter 9, p. 56.
9. G. F. Morrison, *Chemical Desulphurisation of Coal* (IEA Coal Research Report ICTIS/TRI5, International Energy Agency Coal Research, London, 1981); D. L. Khoury, *Coal Cleaning Technology* (Noyes Data Corporation, Park Ridge, N.J., 1981).
10. Z. Hussain, E. Umbach, D. A. Shirley, J. Stohr, J. Feldhaus, *Nucl. Instrum. Methods*, **195** 115 (1982).
11. F. W. Lytle *et al.*, *ibid.*, in press.
12. J. A. Bearden and A. F. Burr, *Rev. Mod. Phys.* **39**, 125 (1967).
13. E. A. Stern and S. Heald, *Rev. Sci. Instrum.* **50**, 1579 (1979).
14. Registered trademark of Chemplex Industries, Inc.
15. D. H. Maylotte, J. Wong, R. L. St. Peters, F. W. Lytle, R. B. Greegor, *Science* **214**, 554 (1981).
16. Analyses of this coal were performed at the Utah International Inc., Sunnyvale Minerals Laboratory, Sunnyvale, Calif. Results of these analyses were as follows: H_2O, 6.91 percent; ash, 7.10 percent; sulfur, 1.44 percent; volatile matter, 36.08 percent; fixed carbon, 49.91 percent; heating content, 12087 British thermal units. Sulfur forms were determined through American Society for Testing and Materials procedure 2492-79.
17. R. Hayatsu, R. G. Scott, L. P. Moore, M. H. Studier, *Nature (London)* **257**, 378 (1975).
18. Recent measurements on a freshly cleaved pyrite mineral specimen by G. E. Brown of Stanford University show that the absorption peak at 11.8 eV in our pyrite specimen was actually due to an oxidation product on the surface of pyrite particles. This impurity which exists in both the pyrite model compound and the coal specimen does not, however, invalidate our conclusion on the nature of the organic sulfur species in the coal examined.
19. We are grateful for experimental opportunities at the Stanford Synchrotron Radiation Laboratory, which is supported by the U.S. Department of Energy.

9 May 1984; accepted 19 June 1984

El Niño–Southern Oscillation Events Recorded in the Stratigraphy of the Tropical Quelccaya Ice Cap, Peru

Abstract. *Snow accumulation measured during 1982–1983 on the Quelccaya ice cap, Peru, was 70 percent of the average from 1975 through 1983. Inspection of 19 years (1964 through 1983) of accumulation measured near the summit of Quelccaya reveals a substantial decrease (~30 percent) in association with the last five El Niño–Southern Oscillation (ENSO) occurrences in the equatorial Pacific. The ENSO phenomenon is now recognized as a global event arising from large-scale interactions between the ocean and the atmosphere. Understanding this extreme event, with the goal of prediction, requires a record of past occurrences. The Quelccaya ice cap, which contains 1500 years of annually accumulated ice layers, may provide a long and detailed record of the most extreme ENSO events.*

The years 1982 and 1983 were characterized by large, coherent climate anomalies over much of the earth (*1*, *2*). Synthesis of atmospheric data (pressure, temperature, and rainfall) and oceanic data (sea-surface temperatures) has led to the view that the El Niño–Southern Oscillation (ENSO) is a large-scale interaction between the atmosphere and ocean in the tropics (*3*). Recently these interactions have been linked with extraordinary weather conditions in diverse locations over the globe (*4*). Understanding these interactions with the goal of predictability requires a long history of past events. Currently this record encompasses 116 years (*5*), of which only the last 60 are well documented.

Results from the glaciological investigation of the tropical Quelccaya ice cap in Peru (*6*) since 1976 indicate that major ENSO occurrences may be recorded on this ice cap in the form of substantially reduced annual snow accumulation. The annual mass balance of this ice cap is an integration of the annual precipitation and radiation balances. The purpose of this report is to examine the temporal relation between the amount of mass accumulation on Quelccaya and these tropical Pacific ENSO events.

Each year since 1976, ~25 water samples representing 1 year of snow accumulation on Quelccaya have been collected for analysis of the microparticle concentration, oxygen isotopic abundance ratios, and beta radioactivity (*7*, *8*). Figure 1 is a composite of the microparticle concentrations in eight pits (1976 through 1983) that are joined to produce a continuous time series. The dry season (July) horizons (Fig. 1), easily identified by visual inspection within the snow pits, result from the concentration of microparticles during the dry season (*7*). The thicknesses of these annual dust layers reflect the annual snow accumulation (Fig. 1, dashed lines). Using measured densities, one can convert snow accumulation into water equivalent accumulation estimates (Fig. 1).

The 8 years of pit data yield an annual average of 1.10 m of water per year. Precipitation was sharply reduced (~30

percent) during 1976–1977 and 1982–1983, both periods of intense ENSO events (*9*). In Fig. 2 we compare the Quelccaya mass balance data (1975 through 1983) (Fig. 2c) with the Southern Oscillation index (the pressure difference between Tahiti and Darwin) (*9*) (Fig. 2a) and annual sea-surface temperature (SST) anomalies at Puerto Chicama, Peru (*1*, *10*) (Fig. 2b). On an annual basis for 8 years (1976 through 1983) positive SST anomalies are significantly correlated ($R = 0.66$; $R^2 = 0.44$; significance level = 93 percent) with a decrease in the snow accumulation (water equiva-

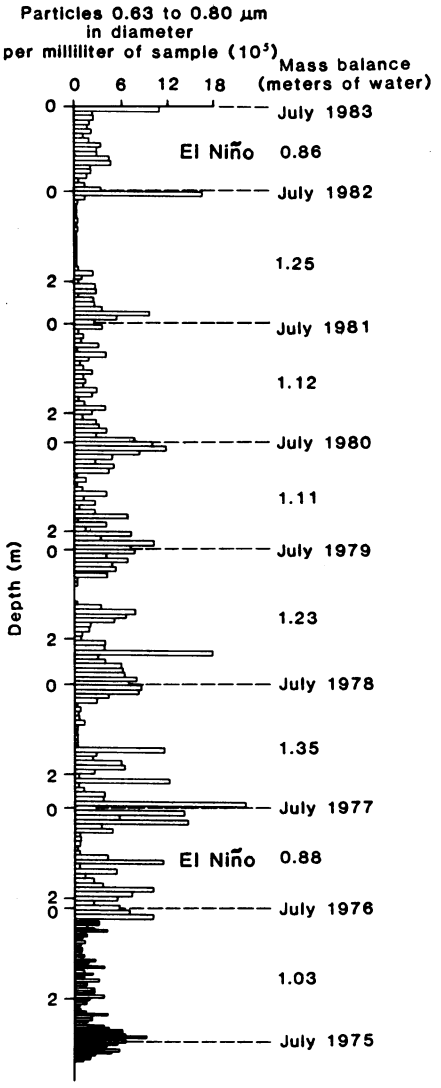

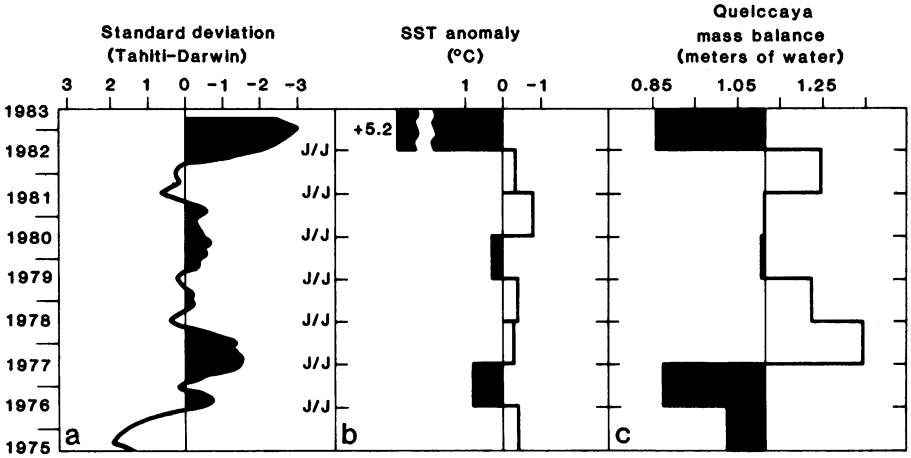

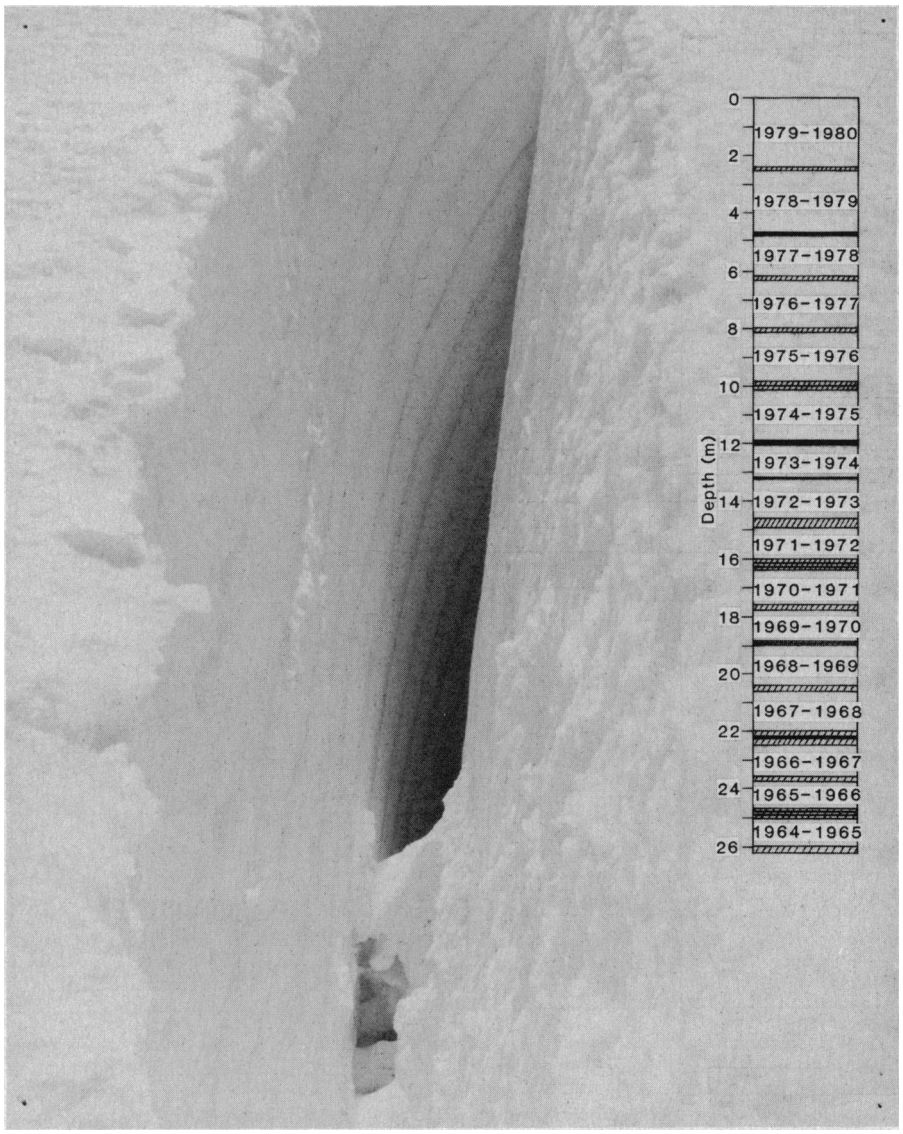

Fig. 1 (left). Small-diameter particle concentrations measured in samples from successive pits on Quelccaya ice cap from 1976 to 1983. High particle concentrations are associated with the dry season from May to August. The dashed line represents the July snow surface, and hence the separation between pairs of these lines represents snow accumulation over the thermal year (July to subsequent June). Mass balance variations are given in meters of water equivalent. The El Niño years of 1976–1977 and 1982–1983 exhibit marked reductions in mass balance. Fig. 2 (top right). Time history (1975 through 1983) of: (a) the atmospheric pressure anomaly at sea level at Tahiti minus that at Darwin (*1*), which is used as a Southern Oscillation index; (b) the annual sea-surface temperature (SST) anomalies (*1*, *10*) [the standard deviations for the SST record are with respect to the 26-year mean temperature of 16.9°C at Puerto Chicama (*10*)]; (c) annual accumulation (in meters of water equivalent) on the summit of Quelccaya as illustrated in Fig. 1. All the data are calculated for the thermal year (July to subsequent June), thus spanning two calendar years. Fig. 3 (bottom right). Photograph (1980) illustrating the stratigraphy within a 26-m crevasse 1 km east of the Quelccaya summit. Looking vertically down into the crevasse, one can view the horizontal dirt layers preserved within the ice cap. The annual layer separations shown on the right were used to calculate the mass balance record presented in Fig. 4.

lent) on Quelccaya. Moreover, a lesser event (1979–1980) (present in pressure and SST records) is modestly recorded on Quelccaya. These data support our 1983 field observation that a physical relation may exist between the amount of snow accumulation on Quelccaya and major ENSO occurrences.

In 1980, samples were collected from the walls of a 26-m crevasse located 1 km east of the ice cap summit. Figure 3 illustrates the excellent visible stratigraphy along the crevasse wall from which a 16-year (1964 through 1980) snow accumulation record was obtained (Fig. 4). The annual average mass accumulation over this period is 0.95 m of water, less than the average for 1975 through 1983 for the summit (1.10 m) because of the lower elevation and correspondingly slightly higher ablation at the site. Although the average accumulations are slightly different for the two sites, the five overlapping years (1975 through 1980) exhibit similar trends about their respective means (summit, 1.12 m year^{-1}; crevasse, 1.00 m year^{-1}). Periods of lower mass balance recorded in the crevasse (Fig. 4c) are better correlated with positive SST anomalies (Fig. 4b) (R = 0.45; R^2 = 0.20; significance level = 92 percent) than with the negative pressure anomalies (Fig. 4a) (R = 0.35; R^2 = 0.15; significance level = 87 percent). The lower mass balance in 1970–1971 is not associated with either ENSO indicator. All data used in the correlation calculations reflect the thermal year (July to subsequent June). These relations may be investigated over a slightly longer time interval if we construct a composite accumulation time series from the crevasse record (1964 through 1980) and the pit records (1981 through 1983). The correlation characteristics for this longer time record are identical to those for the period from 1964 through 1980.

The reduced annual accumulation on Quelccaya recorded at the summit (pit data) and in the stratigraphic record of the crevasse is thus temporally correlated with two prominent indicators of major ENSO events. This relation suggests that meteorological conditions governing the annual abundance of snowfall on the Quelccaya ice cap may be physically linked to the major climate anomalies (ENSO events) in the equatorial Pacific. In addition, the precipitation on Quelccaya originates over the Amazon Basin to the east; thus there may be a link between meteorological processes over the Amazon Basin and equatorial Pacific ENSO events.

The potential relation between these ENSO events and Quelccaya mass balance may prove especially valuable since two ice cores drilled at the Quelccaya summit in 1983 contain 1500 years of annual deposited ice layers. The 1500-year record of estimated annually accumulation that will be extracted from these cores may provide an equally long record of major ENSO occurrences. Equivalent records of microparticle concentrations and size distribution, oxygen isotopic abundance ratios, and specific conductivity will also be available. If these ice core parameters exhibit signals peculiar to ENSO events, one would then have further confidence in the record extracted from the ice cores. The high temporal resolution available in tropical ice cores from carefully selected sites makes them a valuable source of atmospheric information when an interpretable record can be extracted.

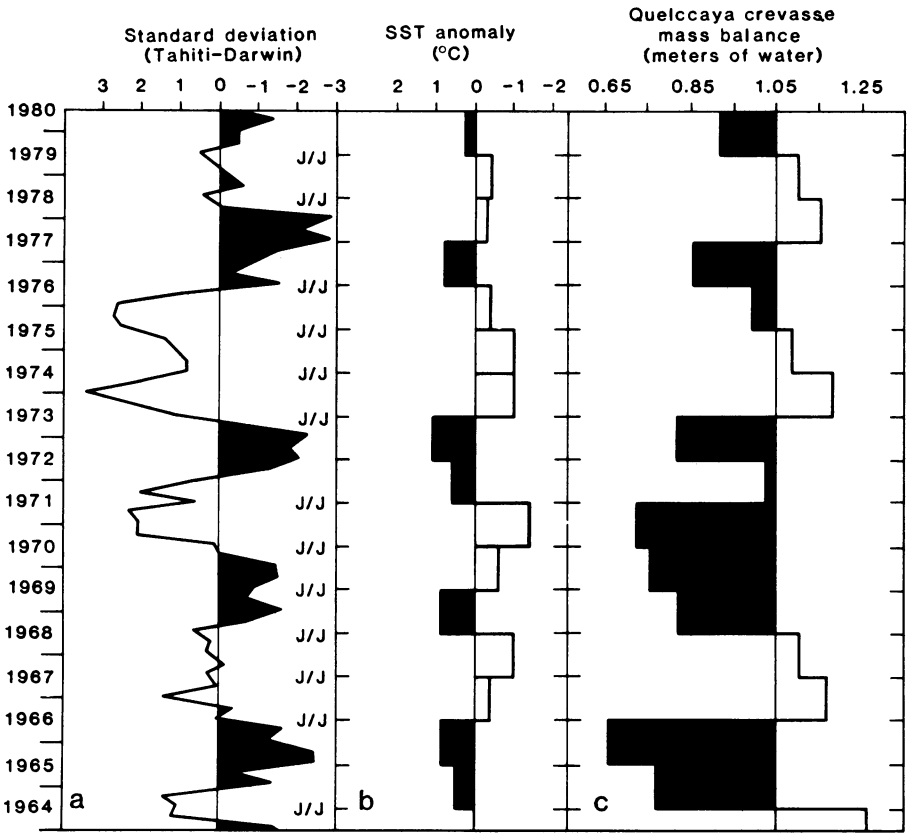

Fig. 4. Time history (1964 through 1980) of: (a) 3-month mean values of the atmospheric pressure anomaly at sea level at Tahiti minus that at Darwin (*11*), used as a Southern Oscillation index; (b) annual SST anomalies (*1*, *10*) [the standard deviations for the SST record are with respect to the 26-year mean temperature of 16.9°C at Puerto Chicama (*10*)]; (c) annual snow accumulations (in meters of water equivalent) (Fig. 3) from the 1980 crevasse 1 km east of the summit. The annual mass balance and SST anomalies are calculated for the thermal year from July to the subsequent June, thus spanning two calendar years, whereas the pressure anomalies are 3-month averages.

LONNIE G. THOMPSON
ELLEN MOSLEY-THOMPSON
Institute of Polar Studies,
Ohio State University,
Columbus 43210
BENJAMÍN MORALES ARNAO
Electroperú,
Lima, Peru

References and Notes

1. E. M. Rasmusson and J. M. Wallace, *Science* **222**, 1195 (1983).
2. M. A. Cane, *ibid.*, p. 1189; D. Halpern, S. P. Hayes, A. Leetmaa, D. V. Hansen, S. G. H. Philander, *ibid.* **221**, 1173 (1983).
3. J. Namias, *J. Phys. Oceanogr.* **6**, 130 (1976); K. Wyrtki, E. Stroup, W. Patzert, R. Williams, W. Quinn, *Science* **191**, 343 (1976); R. L. Smith, *ibid.* **221**, 1397 (1983); E. M. Rasmusson and T. H. Carpenter, *Mon. Weather Rev.* **111**, 517 (1983).
4. E. M. Rasmusson and J. M. Hall, *Weatherwise* **36**, 166 (1983); R. S. Quiroz, *Mon. Weather Rev.* **111**, 1685 (1983).
5. W. H. Quinn, D. O. Zopf, K. S. Short, R. T. W. Kuo Yang, *Fish. Res. Bull.* **76**, 663 (1978).
6. The Quelccaya ice cap (13°56'S, 70°50'W) is in the Cordillera Oriental of southern Peru and has a summit elevation of 5670 m above sea level. The ice cap is on the extreme western edge of the Amazon Basin.
7. L. G. Thompson, E. Mosley-Thompson, P. Grootes, M. Pourchet, S. Hastenrath, *J. Geophys. Res.* **89**, 4638 (1984).
8. L. G. Thompson, *Ohio State Univ. Inst. Polar Stud. Rep. 64* (1977).
9. A. E. Gill and E. M. Rasmusson, *Nature (London)* **306**, 229 (1983).
10. R. T. Barber and F. P. Chavez, *Science* **222**, 1203 (1983).
11. J. Rogers, personal communication.

12. This research was supported by the National Science Foundation Division of Atmospheric Sciences (grants ATM95-15513A02, ATM-7821609A01, ATM-8105079A02, and ATM-8213601A01). We appreciate the support by the National Science Foundation Division of Polar Programs for the initial 1974 field investigation (GV41411) and for development of the solar-

powered drill (designed by the Polar Ice Coring Office, Lincoln, Nebraska) used on Quelccaya in 1983 to obtain two cores, one to bedrock. We are indebted to numerous scientists, engineers, and technicians from Electroperú (Lima and Huaraz offices) who provided both scientific and logistical assistance essential to the success of this 8-year effort. Logistical support was also provided by the Inter American Geodetic Survey (U.S. Defense Mapping Agency) office in Lima, and we especially thank W. Berk. Over 8 years many people have participated in the annual field programs, and their collective efforts are gratefully acknowledged. We thank J. Bolzan and P. D. Kruss for reviewing the manuscript and R. Tope for the illustrations. Contribution No. 509 of the Institute of Polar Studies, Ohio State University.

16 April 1984; accepted 11 May 1984

Temperature Effects on the Rate of Ty Transposition

Abstract. *An assay has been developed to measure the rate of transposition of the transposable element Ty in* Saccharomyces cerevisiae. *The assay is based on the altered expression of the glucose-repressible alcohol dehydrogenase gene of yeast upon insertion of a Ty in front of this gene. By this assay the transposition rate of Ty elements was found to increase approximately 100-fold at temperatures lower than 30°C, the optimum growth temperature for* Saccharomyces cerevisiae.

Ty elements comprise a family of homologous transposable DNA sequences present in about 30 copies in most laboratory yeast strains (*1*, *2*). These sequences are about 5.9 kilobases (kb) long with direct repeats of 330 base pairs called δ sequences at each end. Their structure has many features in common with the *Drosophila* transposable element *copia* and with retroviruses (*1*, *2*). Attempts to measure transposition frequencies with the use of marked elements have not been successful because of the difficulty of distinguishing transposition events from gene conversion of endogenous Ty elements (*3*). To avoid this difficulty, we used a method for detecting transposition of Ty elements based on the ability of Ty elements to alter the expression of adjacent genes (*1*, *2*) and, in particular, the alcohol dehydrogenase 2 (*ADH2*) gene. *Saccharomyces cerevisiae* has three ADH isozymes: ADHI, the fermentative isozyme; ADHII, an isozyme repressible by glucose; and ADHIII, an isozyme associated with mitochondria (*4*). Medium containing antimycin A can be used to select for cells with ADH activity because it eliminates respiration, thus requiring cells to use their fermentative pathway and therefore ADH activity to grow (*4*). Mutants that express ADHII constitutively because of mutations at *ADH2* (the ADHII structural gene) or at regulatory loci for *ADH2* have been selected from a strain lacking ADHI by their ability to grow on medium containing glucose and antimycin A (*4*). Seven of the nine ADHII constitutive mutants selected that were linked to *ADH2* were shown to carry Ty insertions upstream from this gene (*5*).

By determining the rate at which antimycin A–resistant mutations occur and the percentage of such mutations which are the result of the insertion of a Ty element adjacent to *ADH2*, the rate at which Ty elements transpose into this region was estimated. A potential problem in the determination of mutation rates in the ADH system is that cells expressing ADH on glucose-containing medium have a shorter doubling time than cells that do not have ADH activity (2 hours and 4 hours per doubling at 30°C, respectively). To circumvent this problem we used the P_0 method, which bases mutation-rate calculations on the proportion of cultures with no mutations (*6*) (see legend to Table 1). Even though use of this method leads to larger variations in mutation rate than estimates by other methods, it eliminates biases due to growth rate differences of mutants.

Mutation rates to antimycin A resistance were determined in several independent experiments for cultures of a strain carrying a deletion in *ADH1*, the structural gene for ADHI (*7*), grown at 15°, 20°, 30° and 37°C. A total of 83 independent antimycin A–resistant mutants was examined. DNA was isolated from each of these mutants, and transfers (Southern) of genomic DNA cut with Bam HI were examined after hy-

Table 1. Determination of mutation rates with the use of strain 315-1D (*adh1–Δ1 ADH2 trp1 his4*). Construction of a yeast strain carrying a deletion of *ADH1* (mutation *adh1–Δ1*) has been described (*7*). Each line in the table represents an independent experiment. For each estimate of the mutation rate to antimycin A resistance, 16 to 18 cultures were grown for six to eight generations at the experimental temperatures, and a small portion of cells from each culture was plated on YEPD medium (yeast extract, peptone, and dextrose) to determine the total number of cells per culture. The remaining cells were plated on YEPD medium containing glucose and antimycin A and incubated at 30°C (*4*). Colonies were counted after growth at 30° for 5 days. Mutation rates are reported as the number of mutations per cell per generation ± the 95 percent confidence interval (*6*). The increase in transposition rate at low temperatures was not due to a burst of Ty transposition when the cells are first placed at low temperatures because only a small number of mutants per culture was seen (the median number of mutants per culture is between 0 and 7 for all experiments). The cells were plated at approximately 10^6 cells per milliliter for cultures grown at 20° and 15°C and at approximately 10^7 cells per milliliter for cultures grown at 30° and 37°C. For 315-1D cells grown at 37°C the estimates of the number of cells per milliliter from hemocytometer counts was ten times higher than estimates from the number of cells that grew on YEPD plates, indicating that only 10 percent of the cells were viable. Hemocytometer counts were only about 10 percent higher than viable counts for 315-1D grown at the other temperatures and for three independent mutants carrying Ty insertions adjacent to *ADH2* grown at 37°, 30°, and 15°C. The detection of Ty insertions is described in the text. DNA was isolated as described (*17*). Transposition rates are reported as the number of transpositions per cell per generation. These transposition rates are minimum estimates because only one mutant from each culture was tested by Southern blot analysis (*8*) for insertion of a Ty element to ensure that all the mutants were independent. The mean number of mutations per culture was less than 3 for all experiments so that sampling errors should not be a major problem. Also, mutants carrying insertions at *ADH2* appeared to grow as fast (or faster than) as most other antimycin A–resistant mutants. Reconstruction experiments in which three mutants carrying Ty insertions adjacent to *ADH2* and strain 315-1D were grown at 37°, 30°, and 15°C and then mixed at appropriate densities (10 to 100 cells per plate for mutants carrying Ty insertions adjacent to *ADH2* and 10^7 to 10^8 cells per plate for 315-1D) showed nearly 100 percent plating efficiency for all three Ty mutants grown at all three temperatures.

Temperature (°C)	Mutation rate to antimycin A resistance*	Mutants with Ty insertions		Transposition rate†
		Fraction	Percent	
15	$(1.1 \pm 1.0) \times 10^{-7}$	5/12	42	2.4×10^{-8}
20	$(1.6 \pm 1.5) \times 10^{-7}$	5/18	28	1.7×10^{-8}
30	$(6.6 \pm 7.4) \times 10^{-9}$	0/7	3	$<7.4 \times 10^{-10}$
	$(6.8 \pm 12.4) \times 10^{-9}$	0/5		$<9.3 \times 10^{-10}$
	$(4.9 \pm 5.4) \times 10^{-9}$	0/11		$<2.7 \times 10^{-10}$
	$(4.7 \pm 3.0) \times 10^{-9}$	1/12		2.1×10^{-10}
37	$(2.4 \pm 3.6) \times 10^{-7}$	0/2	0	$<1.2 \times 10^{-7}$
	$(1.7 \pm 1.2) \times 10^{-7}$	0/16		$<4.9 \times 10^{-9}$

*Mutation rates were estimated by the P_0 method ($P_0 = e^{-m}$, where P_0 is the number of cultures without mutants and m is the mean number of mutations per culture; m is then divided by the mean number of cells per culture to give the mutation rate) (*6*). †Transposition rates were calculated whereby P_0 is equal to the number of cultures without antimycin A–resistant mutations plus the number of cultures in which the mutant analyzed did not contain a Ty insertion as P_0.